International Journal of Chemical, Materials and Biomolecular Sciences
ISSN: 2415-6620
Vol:10, No:5, 2016

Preparation of Nanophotonics $LiNbO_3$ Thin Films and Studying Their Morphological and Structural Properties by Sol-Gel Method for Waveguide Applications

A. Fakhri Makram, Marwa S. Alwazni, Al-Douri Yarub, Evan T. Salim, Hashim Uda, Chin C. Woei

***Abstract*—**Lithium niobate ($LiNbO_3$) nanostructures are prepared on quartz substrate by the sol-gel method. They have been deposited with different molarity concentration and annealed at 500°C. These samples are characterized and analyzed by X-ray diffraction (XRD), Scanning Electron Microscope (SEM) and Atomic Force Microscopy (AFM). The measured results showed an importance increasing in molarity concentrations that indicate the structure starts to become crystal, regular, homogeneous, well crystal distributed, which made it more suitable for optical waveguide application.

***Keywords*—**Lithium niobate, morphological properties, Pechini method, thin film.

I. Introduction

LITHIUM NIOBATE ($LiNbO_3$) is presented as an important ferroelectric material. Its excellent piezoelectric, electro-optical, pyroelectrical, and photo-refractive, properties made it very attractive material for integrated optics and photonic applications [1]-[5]. It is also employed in nonlinear optics for frequency conversion and in telecommunication for electro-optic modulation [6]-[10]. Recently for optical devices, due to their mechanical robustness, good availability, optical homogeneity, this crystal plays an important role as a high quality source material with low optical loss [11]-[14]. Thin films of nanophotonic $LiNbO_3$ have been studied for use in an integrated form with unique pyroelectric, piezoelectric, and nonlinear optical properties, which would make it an ideal material for the fabrication of surface acoustic wave (SAW) [15], optoelectronic, and optical devices [16].

$LiNbO_3$ thin films were prepared using various experimental techniques such as sputtering [17], [18], sol-gel [19], [20], liquid phase epitaxial (LPE) [21], metal organic chemical vapor deposition (MOCVD) [22]-[24], soft-chemistry [25], hydrothermal methods [26], and pulsed laser deposition (PLD) [27], [28].

This paper reports on the production of LiNbO3 nano and micro photonic crystal by utilizing the Pechini route (Sol-gel). The phase evolution with the molarities concentration was also studied by using XRD, SEM and AFM because it is the important part of our work and application on Optical waveguides from thin film nanoparticles $LiNbO_3$ nano- and micro-photonics.

II. Experimental Procedure

The preparation procedure of $LiNbO_3$ nanostructures is Nb_2O_5 (ultra-purity, 99.99%) and oxalic acid (A.P.) are used without further purification. The solution is prepared by mixing Li_2CO_3, Nb_2O_5, citric acid, and ethylene glycol. The molar ratio between Li_2CO_3 and Nb_2O_5 was 1:1 in order to maximize the formation of $LiNbO_3$ stoichiometry phase. Firstly, the $LiCO_3$, Nb_2O_5, and citric acid were dissolved in Ethylene Glycol with heating and stirring at 90◦C for 8 hours, then mixed all together with continued heating and stirring at 90°C for 8 hours. To obtain homogeneous and crack-free films of $LiNbO_3$, the precursor was deposited by spin coating technique on quartz substrates at a spinning speed of 3000 rpm for 30 sec. Seven layers were prepared, the film was dried at 120°C for 10 min and was annealing (calcined) at 500°C for 2 hours in static air and oxygen atmosphere to remove the organics. The structural evolution of the as-prepared nanophotonics was examined using high-resolution X-ray diffraction (HR-XRD), (X'Pert Pro MRD PW3040 system diffractometer, PANalytical Company, Netherlands) equipped with Cu-K α-radiation of wavelength $\lambda = 0.15418$ nm at 40 kV and 30 mA. The scanning electron microscopy (SEM) (JOEL JSM-6460LV, Oxford instruments, Analytical Ltd., Japan) was used to investigate the surface morphology of $LiNbO_3$, and atomic force microscopy (AFM) (SPM-9600, Scanning Probe Microscope, Shimadzu, Japan) was utilized for investigating the roughness of $LiNbO_3$. The thickness of the annealed samples was studied using scanning optical Reflectometer model (Filmetrics F20, China).

A. Fakhri Makram, Al-Douri Yarub, Hashim Uda are with the Institute of Nano Electronic Engineering (INEE), University Malaysia Perlis (UniMAP), Perlis, Malaysia (e-mail: mokaram_76@yahoo.com, yarub@unimap.edu.my, uda@unimap.edu.my).

Marwa S.Alwazni is with the Laser and Optoelectronic Department, University of Technology, Baghdad, Iraq (phone: +9647702518364; e-mail: malwazny@yahoo.com).

Evan T. Salim is with the Laser Science Branch, University of Technology, Baghdad, Iraq (e-mail: evan_tarq@yahoo.com).

Chin C. Woei is with the Institute of Nano Electronic Engineering (INEE), University Malaysia Perlis (UniMAP), Perlis, Malaysia.

III. Result and Dissection

A. Structural Properties

The crystalline structure of $LiNbO_3$ nanophotonics was found to have hexagonal structure. It is observed from Fig. 1 that the peaks at 2θ = 23.634, 32.637, 34.674, 48.355, 53.106, and 55.879 corresponding to (012), (104), (110), (024), (116) and (122) planes. Therefore, the film structure will be more crystalline with increasing molarity concentration as shown in Fig. 2. The measured structural properties of $LiNbO_3$ nanophotonics were listed in Table I. Crystallite size (D) was calculated using Scherrer's formula (1) [29].

$$D = K\,\lambda/\beta \cos\theta \quad (1)$$

where K is a constant taken to be 0.94, λ is the wavelength of X-ray used (λ = 1.54 Å), β is the full width at half maximum of XRD pattern and θ is Bragg's angle, around 26.41°. In addition, the dislocation density (δ) and strain (ε) of $LiNbO_3$ nanophotonics were determined using the following relations (2), (3) [29].

$$\delta = 1/D2 \quad (2)$$

$$\varepsilon = \beta / 4 \tan\theta \quad (3)$$

The interplanar distance (d) was calculated for all sets of $LiNbO_3$ nanophotonics using Bragg's formula (4) [30].

$$d = h\,\lambda/2 \sin\theta \quad (4)$$

where (h) is a positive integer for hexagonal structure and (d) is an interplanar distance as given in Table I.

The lattice parameters a and c were calculated by (5) [30]

$$\frac{1}{d^2} = \frac{4}{3}\left(\frac{h^2+hk+k^2}{a^2}\right) + \frac{l^2}{c^2} \quad (5)$$

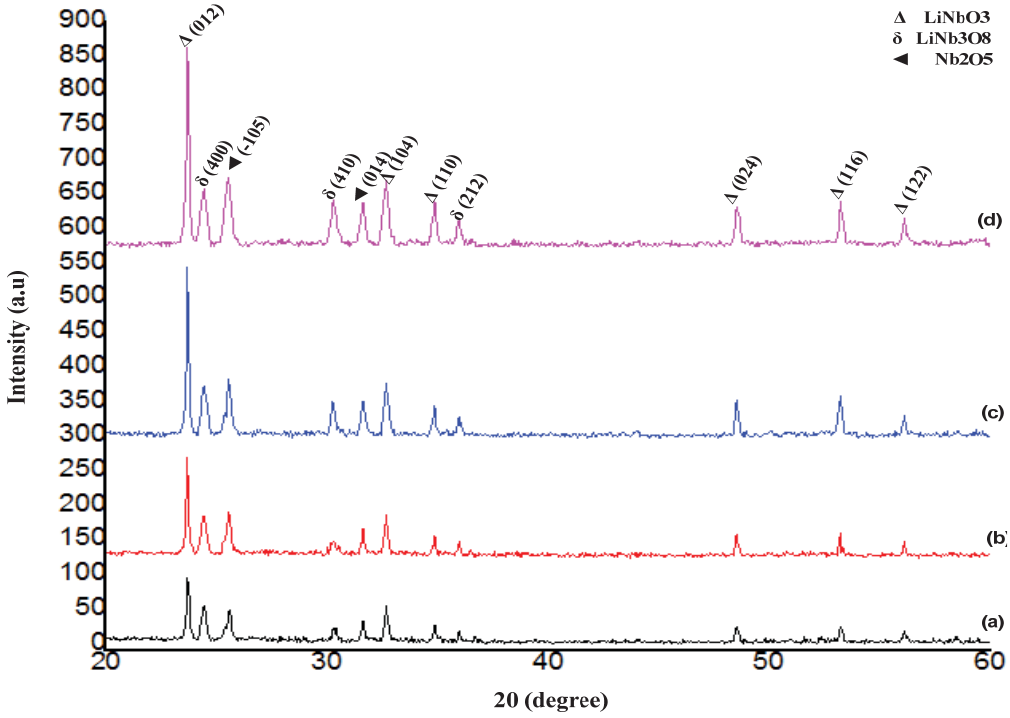

Fig. 1 XRD patterns of $LiNbO_3$ nanophotonics with different molarity concentrations: (a) 0.25 Mol/L, (b) 0.5 Mol/L, (c) 0.75 Mol/L and (d) 1 Mol/L

Fig. 1 shows the XRD pattern obtained from $LiNbO_3$ nanophotonics deposited on quartz substrates. All the peaks indicate to the hexagonal structure with lattice parameters a = b = 5.1566, c = 13.858, which were very close to the reported data in [19]. The nanophotonics have polycrystalline structure annealed at 500°C for 2 h in static air, two phases of $LiNbO_3$ could be recognized, Δ and δ. Δ phase was found to be more preferred despite that it has (012) orientation. The XRD clearly indicates the presence of a small amount of secondary Li deficient phase ($LiNb_3O_8$) at all molarity concentrations. This phase is originated from an interface reaction between the oxygen and $LiNbO_3$, that could be detected by XRD due to its high crystallization temperature at peaks 2θ = 24.407, 30.262 and 35.981 correspond to (400), (410) and (212) planes. There were an impurity like Nb_2O_5, where detected as shown at peaks 2θ = 24.433 and 31.623 correspond to (-105) and (014) planes.

The measured lattice constants had showed good agreement with experimental values as given in Table I.

TABLE I
THE $LiNbO_3$ NANOPHOTONICS PARAMETERS AT 3000 RPM COATING SPEED AND ANNEALED AT 500 °C FOR 2 HOURS USING XRD DATA

Concentration Mol/L	Orientation hkl	Peak (θ)	Particle size (nm)	Dislocation density (δ) (10^9) (lines/m^2)	Strain (10^{-3})	d_{hkl} (Å)	Lattice constants a and c (Å)	Roughness (nm)
0.25	012	23.634	128.195	6.085	1.764	3.76152	a=5.1566, c=13.85	10.6
	104	32.637	116.644	7.350	1.681	2.740457	a=5.1566, c=13.85	
	110	34.674	102.744	9.473	1.182	2.583967	a=5.1566, c=13.85	
	024	48.355	107.506	8.653	0.836	1.880044	a=5.1566, c=13.85	
	116	53.106	97.410	10.539	2.954	1.722497	a=5.1566, c=13.85	
	122	55.879	82.754	14.602	2.783	1.6434	a=5.1566, c=13.85	
0.50	012	23.709	100.213	9.957	1.758	3.748	a=5.1566, c=13.85	12.9
	104	32.701	111.105	8.292	2.516	2.735	a=5.1566, c=13.85	
	110	34.824	93.393	11.465	2.353	2.573	a=5.1566, c=13.85	
	024	48.516	98.680	10.269	1.092	1.874	a=5.1566, c=13.85	
	116	53.230	83.507	13.340	3.436	1.719	a=5.1566, c=13.85	
	122	56.123	75.570	17.511	1.384	1.637	a=5.1566, c=13.85	
0.75	012	23.709	87.213	13.147	1.757	3.748	a=5.1566, c=13.85	15.4
	104	32.701	102.210	9.572	1.258	2.735	a=5.1566, c=13.85	
	110	34.824	79.089	15.987	1.569	2.573	a=5.1566, c=13.85	
	024	48.516	84.544	13.991	1.365	1.874	a=5.1566, c=13.85	
	116	53.230	80.970	15.253	0.736	1.719	a=5.1566, c=13.85	
	122	56.123	72.678	18.932	1.846	1.637	a=5.1566, c=13.85	
1	012	23.709	84.213	14.101	1.757	3.748	a=5.1566 5.1561 5.49340 [31] c=13.85 [32] 13.8669 [31]	16.0
	104	32.701	98.658	10.274	1.677	2.735	a=5.1566, c=13.85	
	110	34.824	77.279	16.745	1.177	2.573	a=5.1566, c=13.85	
	024	48.516	81.544	15.039	1.365	1.874	a=5.1566, c=13.85	
	116	53.230	78.581	16.194	1.375	1.719	a=5.1566, c=13.85	
	122	56.123	70.678	20.018	1.846	1.637	a=5.1566, c=13.85	

B. Morphological Properties

1. SEM

It is a very interesting parameter for integrated-optic and optoelectronic applications. Fig. 2 shows SEM images (5*5 μm) of $LiNbO_3$ nanostructures deposited on quartz substrates at different molarity concentrations. Since the density of nucleation for the $LiNbO_3$ thin films was not uniformly distributed on the flat substrate with different molarity concentration. At least molarity concentrations note that the emergence of a high proportion of the pores and voids, these pores as a result of these impurities impact like Nb_2O_5, the $LiNbO_3$ thin films grew smoothly at higher molarity concentration that leads to perfect distribution better than the lower molar concentration Fig. 1. On the other hand, the structure is more homogenous at higher molar concentration. As discussed earlier, this suggests that higher molarity concentration leads to increase in regular distribution of $LiNbO_3$ nano and micro structures

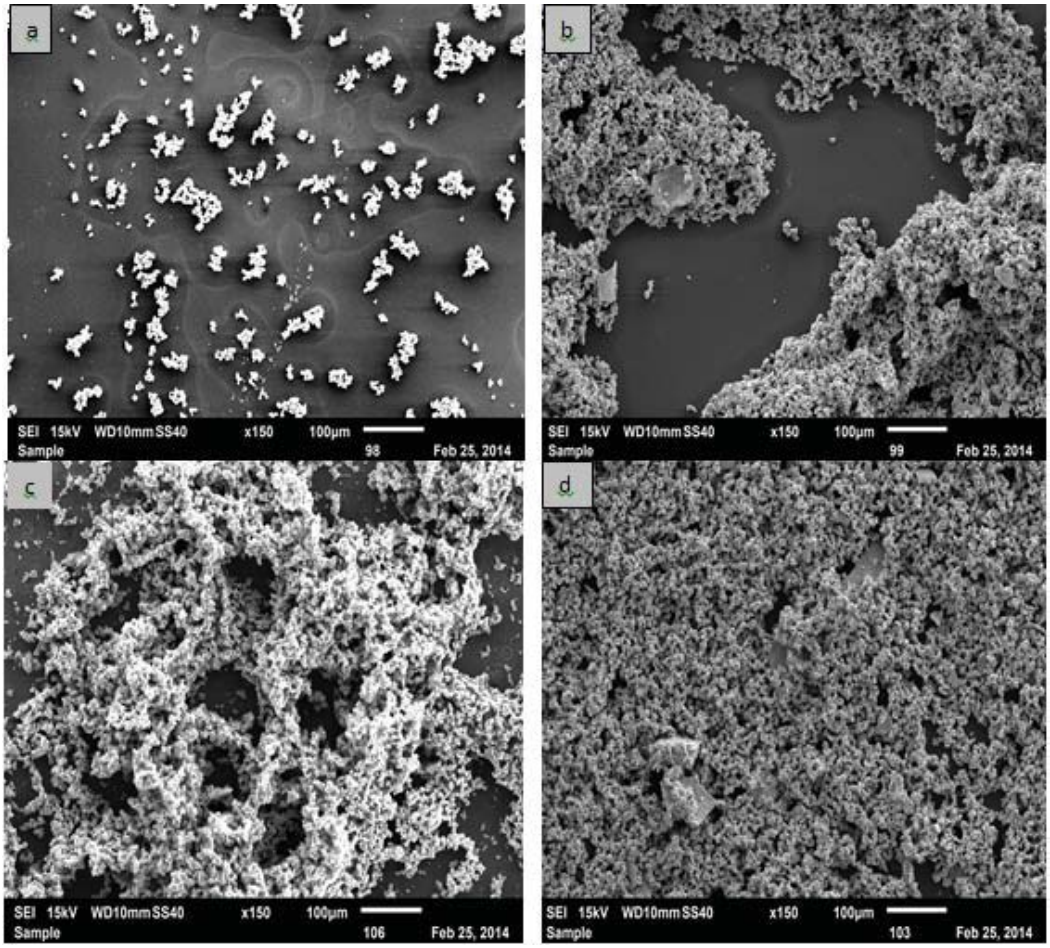

Fig. 2 Surface morphology of $LiNbO_3$ nanostructures at different molarity concentrations. (a) 0.25 Mol/L, (b) 0.5 Mol/L, (c) 0.75 Mol/L and (d) 1 Mol/L

2. AFM

The grain size and root meant square could be affected by molarity concentration. Fig. 3 shows AFM images of the $LiNbO_3$ nanostructures with uniform dense surface and exhibits a decrease in grain size as the molarity concentration increases. The surface topography of $LiNbO_3$ nanostructures as observed from the AFM micrographs proves that the grains are uniformly distributed within the scanning area (5 µm x 5 µm), with individual columnar grains extending upwards. This surface characteristic is quoted from the topographic images that found at 1.00 Mol to be uniform, smooth, and more homogeneous than others. In association with the increase of the average diameter of grain size from 84 to 128 nm, large grains appear on the proportion of solvent Fig. 3 (a). On the other hand, we note that the surface roughness increases as the molarity concentration increase because of the lack of solubility and inversely correlation with grain size. So, the roughness is ranging between 10.6 –16.0 nm. Also, the average surface roughness was sufficiently leveled to prepare the devices.

The thickness was determined using an optical reflectometer. In the same time, the thickness increases as the molarity concentration increase, which leads to increase the deposition process and number of atoms as shown in Fig. 4, the increasing molarity affects negatively on the grain size that guides to smoothen the surface.

IV. Conclusion

The $LiNbO_3$ nanostructures have been chemically prepared by spin-coating technique. Based on XRD results, the $LiNbO_3$ nanophotonics have polycrystalline in nature. The highest intensity shown at orientation (012) at $2\theta = 23.634$, a significant increasing as the spin coating speed at 3000 rpm. As expected, the structure is more crystalline as the molarity concentration increases. Also, SEM explains the nanostructures will be more homogenous as the molarity concentration increases. Morphology gives homogeneity, topography shows gain size decreasing from 128 to 84 nm and roughness is ranging between 10.6 – 16.0 nm as molarity increase due to the lack of solubility and inversely correlated with grain size. The result explained that the highest value of molarity concentrations are more appropriate for optical waveguide.

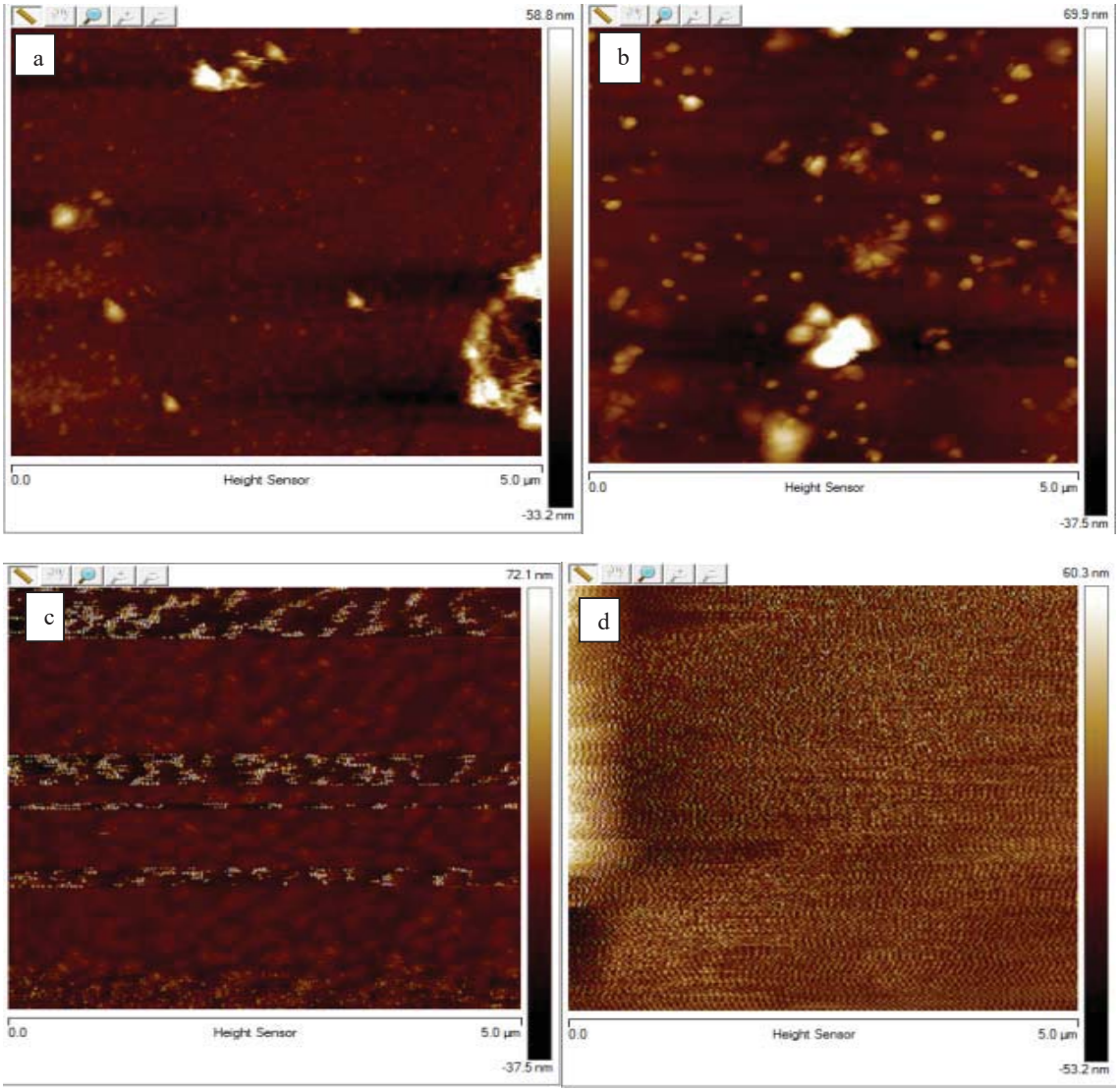

Fig. 3 AFM images of $LiNbO_3$ nanostructures at different molarity concentrations. (a) 0.25 Mol/L, (b) 0.5 Mol/L, (c) 0.75 Mol/L and (d) 1 Mol/L

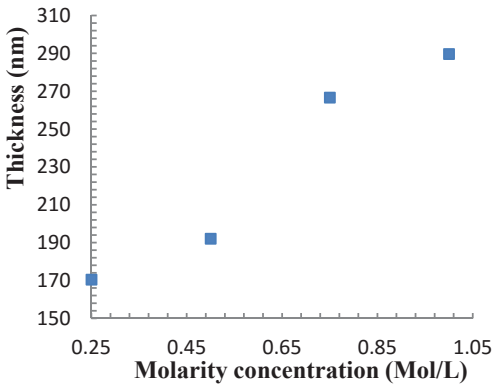

Fig. 4 Thickness of $LiNbO_3$ nanostructures at at different molarity concentrations and at room temperature

REFERENCES

[1] M. A. Fakhri, Y. Al-Douri, U. Hashim,E. T. Salim,"Annealing Temperature Effects on Morphological and Optical Studies of Nano and Micro Photonics Lithium Niobate using for Optical Waveguide Applications " Australian Journal of Basic and Applied Sciences, vol. 9, pp.128-133., 2015.

[2] M. A. Fakhri, Y. Al-Douri, U. Hashim, E. T. Salim, "Optical investigations of photonics lithium niobate", Solar Energy, vol. 120, pp. 381-388, 2015.

[3] Young-Bae Park and Bumki Min et al "Integration of Single-Crystal $LiNbO_3$ thin Film on Silicon by Laser Irradiation and Ion Implantation–Induced Layer Transfer", Adv. Mater, vol. 18, pp. 1533–1536, 2006.

[4] Xinchang Wang and Zhizhen Ye et al "Growth of textured $LiNbO_3$ thin film on Si (111) substrate by pulsed laser ", International Journal of Modern Physics B, Vol. 16, pp.4343-4346, 2002.

[5] Yunbo Guo and Charles Divin et al "Sensitive molecular binding assay using a photonic crystal structure in total internal reflection " Opt Express, vol. 16, pp. 11741–11749, 2008.

[6] Carlos A. Diaz-Moreno and Rurik Farias-Mancilla et al "Structural Aspects $LiNbO_3$ Nanoparticles and Their Ferromagnetic Properties " Materials, vol. 7, pp. 7217-7225, 2014.

[7] Liang Cao and Abdelsalam Aboketaf et al "Hybrid amorphous silicon (a-Si:H)–$LiNbO_3$ electro-optic modulator", Optical Communication, Vol 330, pp. 40–44, 2014.
[8] Hongyun Chen and Tao Lv et al "Discrete diffraction based on electro-optic effect in periodically poled lithium niobate ",optical communication, vol. 294, pp. 202–207, 2013.
[9] H. Hu and R. Ricken, et al "Lithium niobate photonic wires " Optics Express, Vol. 17, pp. 24261-24268, 2009.
[10] Abd El–Naser A. Mohamed and Mohamed A. Metawe'e "Ultra High Speed Semiconductor Electrooptic Modulator Devices for Gigahertz Operation in optical communication Saystems ", International Electrical Engineering Journal(IEEJ), Vol 2, pp. 560-570, 2011.
[11] P. Galinettoa and M. Marinonea et al "Micro-Raman analysis on $LiNbO_3$ substrates and surfaces: Compositional homogeneity and effects of etching and polishing processes on structural properties" Optics and Lasers in Engineering, Vol. 45, pp. 380–384, 2007.
[12] Tao Zhang and Biao Wang et al "Optical homogeneity and second harmonic generation in Li-rich Mg-doped $LiNbO_3$ crystals ", material chemisty and physics, Vol. 88, pp. 97-101, 2004.
[13] Wooten, E.L and Kissa, K.M "A eview of Lithium Niobate Modulators for Fiber-Optic Communications Systems ", IEEE Journal of Selected Topics in Quantum Electronics, Vol. 6, pp . 69-82, 2000.
[14] Woo-Kyung Kim and Soon-Woo Kwon et al "Integrated optical modulator for signal upconversion over radio-on-fiber link ", Optics Express (C), Vol. 17, pp: 2638 -2645, 2009.
[15] Rong Lin and Yuanmei Gao et al " Factors that influence the modulation instability in self-defocusing photorefractive crystal "optical communication, Vol. 285, pp. 2724–2728, 2012.
[16] Jianping Guo, and Jiahu Zhu et al "A plasmonic electro-optical variable optical attenuator based on side-coupled metal–dielectric–metal structure ", Optical Communication, vol. 294, pp: 405–408 2013.
[17] O. P. Nautiyal and S. C. Bhatt "Preparation and Characterization of Lithium Doped Silver Niobate Perovskite System "American Journal of Materials Science vol.1 , pp, 1-4, 2011.
[18] V. Iyevlev and A. Kostyuchenko "preparation and characterization of $LiNbO_3$, grown by RF magnetron sputtering", Journal of material science : Material in electronics, vol.22, pp. 1258-1263, 2011.
[19] A.Z. Simo˜es and M.A. Zaghetea "$LiNbO_3$ thin films prepared through polymeric precursor method ", Materials Letters, Vol 57, pp. 2333–2339, 2003.
[20] A.Z. Simo˜esa, and M.A. Zaghete et al "Influence of oxygen atmosphere on crystallization and properties of $LiNbO_3$ thin films", Journal of the European Ceramic Society, Vol. 24, pp.1607–1613, 2004.
[21] L. H. Wang and D. R. Yuan et al " Synthesis and characterization of fine lithium niobate powders by sol- gel method", Cryst. Res. Technol, vol. 42, pp, 321 – 324, 2007.
[22] Yi Lu and Peter Dekker "Growth and characterization of lithium niobate planar waveguides by liquid phase epitaxy ", journal of crystal growth , vol. 311, pp. 1441–1445 .
[23] Yasunobu Akiyama and Katsuya Shitanaka et al, "Epitaxial growth of lithium niobate film using metalorganic chemical vapor deposition", Thin Solid Films, vol. 515, pp, 4975–4979, 2007.
[24] Akira Tanaka and Keiji Miyashita et al "Preparation of lithium niobate films by metalorganic chemical vapor deposition with a lithium alkoxide source ", Journal of crystal growth, vol. 148, pp. 324–326, 1995.
[25] Sang-Chul Jung and Nobuyuki Imaishi, " The growth of $LiNbO_3$ thin film by LPMOCVD using β-diketonate complexes ", Korean Journal of Chemical Engineering, vol. 16, pp. 229-233, 1999.
[26] May Nyman and Travis M Anderson at al, "Comparison of Aqueous and Non-aqueous Soft-Chemical Syntheses of Lithium Niobate and Lithium Tantalate Powders ", Cryst. Growth Des, vol. 9, pp: 1036–1040, 2009.
[27] Ryo Ageba and Yoichi Kadota et al, "Ultrasonically-assisted Hydrothermal Method for Ferroelectric Material Synthesis " Journal of the Korean Physical Society. vol 57, pp: 918_923, 2010.
[28] Yu-Jin Kang and Se-Young Jeong et al, "Hetero-Epitaxial Growth of $LiNbO_3$ Thin Film on GaN/Al_2O_3 by Pulsed Laser Deposition ", Journal of the Korean Physical Society, vol. 49, pp. S625_S628, 2006.
[29] M. A. Fakhri, Y. Al-Douri, U. Hashim, E. T. Salim, Deo Prakash, K. D. Verma, " Optical investigation of nanophotonic lithium niobate-based optical waveguide", Applied physics B Lasers and Optics, vol. 121, pp. 107-116, 2015.
[30] M. A. Fakhri, Y. Al-Douri, U. Hashim, E. T. Salim, "XRD Analysis and Morphological Studies of Spin Coated $LiNbO_3$ Nano Photonic Crystal Prepared for Optical Waveguide Application", Advanced Materials Research, vol. 1133, 457-461, 2016.
[31] I.-K. Jeong, "Correlated Thermal Motion in Ferroelectric $LiNbO_3$ Studied Using Neutron Total Scattering and a Rietveld Analysis", Journal of the Korean Physical Society, vol. 59, pp. 2756-2759, 2011.
[32] A.Z Simões, A.H.M González, A.A Cavalheiro, M.A Zaghete, B.D Stojanovic, J.A Varela, "Effect of magnesium on structure and properties of $LiNbO_3$ prepared from polymeric precursors", Ceramics International, vol. 28, 265–270, 2002.